ISSN: 2834-7706

Research Article

Journal of Mathematical Techniques and Computational Mathematics

El Niño Impacts on the Ozone Column Over Mato Grosso Do Sul

Amaury de Souza[1]* Umesh C. Dumka[2], Ivana Pobocikova[3], José Francisco de Oliveira-Júnior[4], Marcel Carvalho Abreu[5], Razika Ihaddadene[6], Guilherme Henrique Cavazzana[7], Carlos José dos Reis[8], Flavio Aristone[9], Sajid Gul[10],[11], Nabila Ihaddadene[12], Munawar Shah[13], Widinei A Fernandes[14]

[1]Federal University of Mato Grosso do Sul, C.P. 549, 79070-900. Campo Grande, MS – Brazil.

[2]Aryabhatta Research Institute of Observational Sciences, Nainital, 263 001, India.

[3]Department of Applied Mathematics, Faculty of Mechanical Engineering, University of Zilina, Slovakia.

[4]Federal University of Alagoas, Institute of Atmospheric Sciences (ICAT), Maceió, Brazil.

[5]Rural Federal University of Rio de Janeiro, Seropédica, Rio de Janeiro, Brasil.

[6]Department of Mechanical Engineering, University of M'Sila, M'Sila 28000, Algeria.

[7]Universidade Católica Dom Bosco – UCDB, Campo Grande, Mato Grosso do Sul, Brasil

[8]Department of Agricultural, Statistics and Experimentation Institution: Department of Statistics, Federal University of Lavras – UFLA-CEP, Brazil. 37200-900.

[9]Federal University of Mato Grosso do Sul, C.P. 549, 79070-900. Campo Grande, MS – Brazil.

[10]Henan Academy of Big Data, Zhengzhou University, Zhengzhou 450052, China.

[11]School of Mathematics and Statistics, Zhengzhou University, Zhengzhou 450001, China.

[12]Department of Mechanical Engineering, University of M'Sila, M'Sila 28000, Algeria.

13Department of Space Science. Institute of Space Technology, Islamabad. Pakistan.

[14]Federal University of Mato Grosso do Sul, C.P. 549, 79070- 900. Campo Grande, MS – Brazil.

[*]Corresponding author:
Amaury de Souza, Federal University of Mato Grosso do Sul, C.P. 549, 79070-900. Campo Grande, MS – Brazil.

Submitted:16 Nov 2022; **Accepted:**26 Nov 2022; **Published:**01 Dec 2022

Citation: *Souza, A. D., Dumka, U. C., Pobocikova, I., Oliveira, J. F. D., Abreu, M. C., et, al. (2022). El Niño Impacts on the Ozone Column Over Mato Grosso Do Sul. J Math Techniques Comput Math, 1(3), 165-175.*

Abstract

The El Niño-South Oscillation (ENSO), a dominant factor in interannual climate variations worldwide, is characterized in the Pacific by anomalous sea surface heating during the El Niño phase and cooling during the La Niña phase. Although ENSO strongly affects atmospheric circulation, its effects on tropospheric ozone are not fully explored. We used satellite measurements of the tropospheric column of ozone to assess the effects of atmospheric circulations driven by ENSO on tropospheric column ozone levels in Mato Grosso do Sul (MS). The objective of this work is to analyze the annual variation and the effects of the El Niño atmospheric variability mode in the Total Ozone Column (TCO) on MS between 2005 and 2020 using data from the AUREA satellite and the \Ozone Monitoring Instrument (OMI) sensor. We found that observed ozone tends to increase in the troposphere after the La Niña peak, corresponding to anomalous downward motions and suppressed convection. The model also reveals that the La Niña-related ozone increase in MS is largely due to intensified transport of ozone-rich air from higher latitudes. This suggests that ENSO should be considered for estimating the ozone concentration in MS, requiring close attention to the properties of ENSO in a changing climate.

Keywords: *El Niño-Southern Oscillation, La Niña, Tropospheric Ozone, Chemistry-Climate, Mato Grosso DO SUL.*

Introduction

Tropospheric ozone is a photochemical pollutant produced from the chemical reaction of its precursors. It can have serious social and economic consequences, including adverse effects on human health and reduced agricultural production [1, 2, 3, 4]. In addition, ozone is a greenhouse gas that absorbs terrestrial longwave radiation and warms the atmosphere despite its short residence time [5].

While tropospheric ozone concentration is mainly controlled by in situ photochemical reactions and net transport from the stratosphere [6]. Some studies have revealed the role of El Niño-Southern Oscillation (ENSO) in large-scale interannual variations of ozone in the tropics. El Niño can cause a decrease in tropospheric ozone in the eastern Pacific and an increase in the western Pacific [7, 8]. This negative (positive) ozone anomaly in the eastern (western) Pacific during El Niño periods can be attributed to increased (suppressed) convection associated with weakened Walker circulation. La Niña generally induces the opposite conditions; with suppressed (increased) convection, tropospheric ozone is increased (decreased) over the eastern (western) Pacific [8-10]. Modeling studies suggest that suppressed convection promotes downward transport of air with higher ozone content from the upper troposphere, thereby increasing tropospheric ozone concentrations [10-12]. In contrast, increased convection and upward movement of ozone-poor air from the surface results in a decrease in tropospheric ozone.

Changes in circulation associated with ENSO events also play a substantial role in inducing interannual tropospheric ozone variability, extending to the extra tropics [13]. Olsen et al. identified a significant link between ENSO and tropospheric ozone in mid-latitudes from satellite-measured ozone assimilation [14]. This link mainly reflects the connection of tropospheric ozone to ENSO-induced anomalous anticyclonic and cyclonic circulations, suggesting that higher and lower tropospheric ozone are attributable to increased and suppressed vertical transport of ozone, respectively. In addition, tropospheric ozone can be transported to other regions via atmospheric circulation, indicating the importance of considering atmospheric conditions in ozone variability analysis [13, 15].

ENSO, a tropical Pacific phenomenon characterized by coupled oceanic (El Niño) and atmospheric (southern oscillation) components, an important source of interannual variability in the atmosphere as well as the distribution of atmospheric tracers, such as stratospheric ozone [16]. More definitions about this phenomenon in [17]. Any modification in lower stratospheric ozone induces potential anomalies in troposphere circulation and temperature that are strong enough to impact the surface [18]. These assessments of the impact of ENSO on the distributions of atmospheric constituents in the tropical region are mainly focused on ozone and water vapor [19, 20]. According to Manatsa and Mukwada, the results indicate that during ENSO extremes the Walker Circulation (CW) and CBD are related to lower changes in stratospheric ozone and consequently in the Total Ozone Column (TCO) eastward in the Pacific [21, 22].

The Atlantic Forest area is an extremely important biome due to its abundant biological diversity and has gained great interest as a conservation area since its biome has been considerably reduced. The Brazilian Cerrado, a vast tropical savanna ecoregion, is widely known for its native habitats and rich biodiversity, and represents the second largest biome in South America, after the Amazon. The Cerrado of Mato Grosso do Sul is in two hydrographic regions of Brazil, Paraná and Paraguay. The Pantanal region is the world's largest inland wetland. It is a home to a rich wildlife and is known for its unique biome, however it is also considered as a biodiversity hotspot due to environmental degradation and damage (Teodoro et al. 2016; Oliveira-Júnior et al. 2020) [2, 3, 23].

Therefore, the objective of this study is to evaluate the variability of TCO on MS in interannual time scales, obtain the average concentration, evaluate regions within the study area with different behavior of variations and analyze the influence of the ENOS variability mode, with emphasis in El Niños no Cerrado in the state of Mato Grosso do Sul in Brazil.

Materials and Methods

Study Area Geography and Meteorology

The state of MS is in the Midwest Region of Brazil (Figure 1a), with approximately 358.159 km2. The State is known for its agricultural activity, the main economic products in MS, in particularly soy and cattle production. The topography (Figure 1b) has elevations ranging from 24 to 1,100 m,while the mean annual temperatures range from 20 to 26°C, and mean annual rainfall ranges from 1,000 mm to 1,900 mm. The state has a well-defined dry season between April and September, in which the highest rainfall records are observed in the southern portion of the state. However, in the rainy season, the northern region of the state receives higher rainfall records in the rainy season (between October and March) compared to the southern region [2, 3, 23].

The Köppen's climate classification divides the climate diversity of MS to several climatic regions: i) "Aw" (in the Southeast and North of the state), ii) "Am" (central region), iii) "Af" (Southwest), and iv) "Cfa" (Southern state) (Figure 1c). In the Southwest of MS, south of the Pantanal (between -21º and -22º latitudes), the climate characterizes as tropical forest ("Af"), with rainfalls distributed throughout the year. The central portion of the state is predominantly characterized by tropical monsoon climate ("Am"), with a small dry season during winter. The North, the small part of the central region and the Southeastern state, the natural climate is savannah ("Aw") which tends to dry winters and rainy summers. Only in the South of the state, the climate is humid with hot summers during all seasons ("Cfa") (temperatures > 22ºC) [24, 25]. The biome diversity of MS, as represented in Figure 1d, includes areas of the Atlantic Forest, Cerrado and Pantanal (encompassed 14%, 61% and 25% of the state's area, respectively). The cities studied in the state of MS were Campo Grande (State capital), Chapadão do Sul, Corumbá, Coxim, Dourados, Ponta Porã, Porto Murtinho and Três Lagoas - (Figure 1). These cities were chosen according to the availability of the O_3 concentration data (DU).

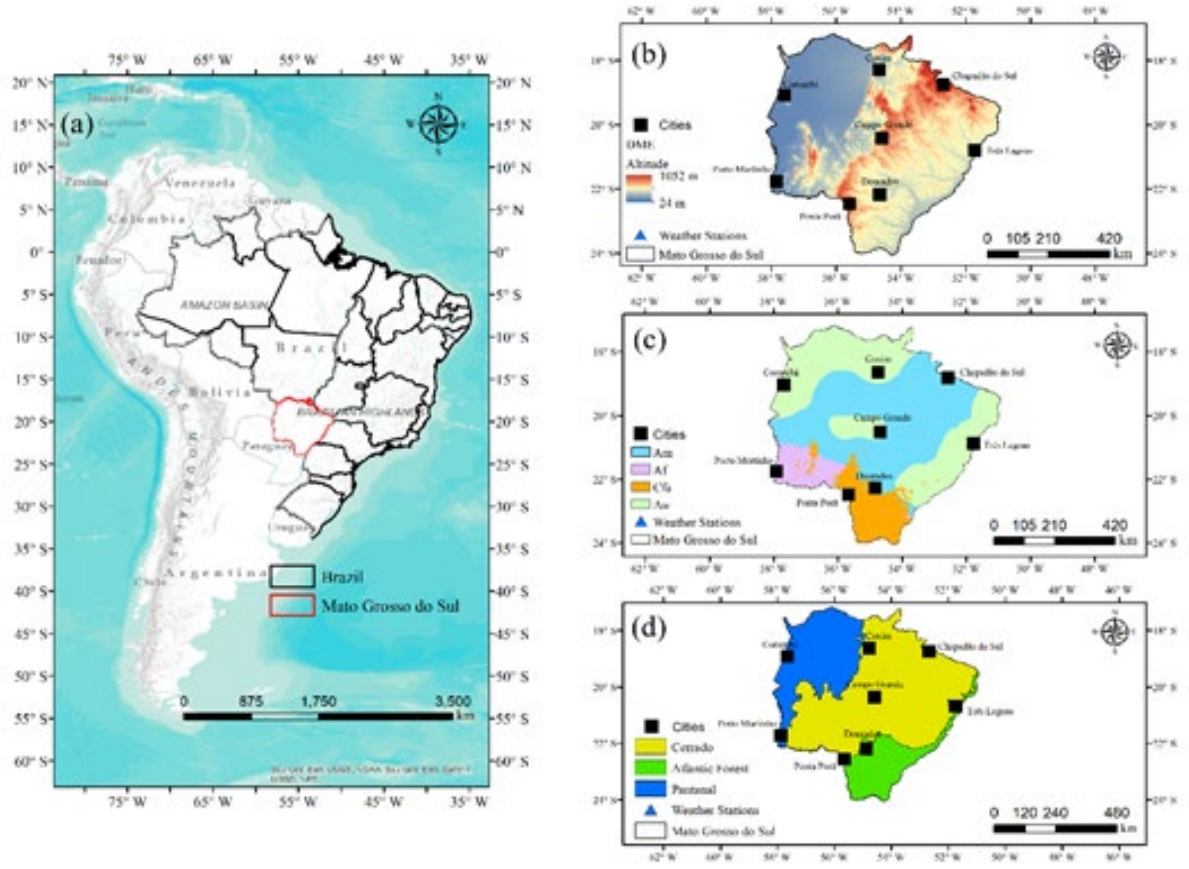

Figure 1

Mato Grosso do Sul state in Brazil (a) and its model digital elevation (MDE) (b), climate classification by Köppen (b) and biomes(d) localization and cities of study.

Satellite Data for O_3

For this work satellite data (AUREA, Ozone Monitoring Instrument - OMI sensor, 0.25-degree resolution and duration in years from 2005 to 2020) are selected. OMI was designed to distinguish the ozone and other atmospheric species including aerosol types such as smoke, dust and sulphates and can measure cloud pressure and coverage, which provide data to derive tropospheric ozone by nadir viewing, wide field imaging UV and visible spectrometer. OMI sensor having spectral region of 264-504 nm, spectral resolution of 0.42nm- 0.63nm and resolution of 0.1250 × 0.1250. The main objective of OMI is to get the global measurements in both troposphere and stratosphere at high spatial and spectral resolution of a number of trace gases [26].

For monitoring the recovery of the ozone layer OMI is the key instrument on EOS Aura in response to the phase out of chemicals, such as CFCs, agreed to by the nations of the world in the Montreal protocol and later modifications to it at Copenhagen, and London. For total ozone measurements OMI effectively continues the TOMS record. OMI technique used by DOAS theory Beer-Lambert Law Measure wavelength dependent light intensity I [λ] as light passes through the air mass. Initial intensity Io [λ] decreases in the air mass due to absorption by the trace gas and scattering by molecules and aerosol particles. Trace gas can be detected in the ratio of I [λ] to Io [λ] as a function of wavelength due to their unique absorption features.

Analysis of Historical Series of Monthly Precipitation

The analysis of the occurrence of ENSO climate variability mode during the period from 2005 to 2020 consisted of plotting the annual totals of the series by extracting its linear trend line and the standard deviation of the series and then comparing the annual totals with the information about the occurrence of the ENSO climate variability mode available on the website of the National Weather Service Climate Prediction Center (NOAA) (http://www.cpc.ncep.noaa.gov). Another way of analyzing the influence of the ENSO climate variability mode on the series' annual rainfall was through the application of the Rain Anomaly Index (RAI), in order to of obtaining the positive and negative anomalies [2, 3, 27].

Results and Discussions

Analysis of interannual variability of TCO in Mato Grosso do Sul

The evaluation of the behavior of the interannual and seasonal variability of the TCO for the entire MS region is presented in Fig. 1. The interannual variability of RAI+ and RAI- for the period between 2005-2020 is represented in Fig. 2 and Fig. 3. The equation of the linear regression line presents a negative angular coefficient, indicating a tendency to decrease the average values of TCO (supplementary Figure 1). It is possible to observe that the TCO values in MS in the analyzed period are typically concentrated between 254 with a minimum average of 260 and a maximum average of 258 with a standard deviation of 2.36 UD and a coefficient of variation of 5.55 DU. The existence of a semi-annual cycle of variation of the TCO was observed, having its minimum values in the April-May-June quarter of each year and the highest in the September-October-November quarters, in line with the study period of 2005 to 2015, similar to what was observed by in the period 2001 to 2009 and in the period from 1978 to 2013 [28, 29, 30]. The semi-annual cycle of the MS region shows the behavior of TCO in each year, the variability of the values found corroborates those obtained by [30]. In this cycle there is not great influence of the ENSO variability modes.

The variation in TCO in MS is not as pronounced as seen in and but it presents a smooth curve with a variation of approximately 6.29 DU, its minimum value in the year 2019 (254.39 UD) and the maximum value in the year 2008 (260.66 UD) [29, 30]. In the years 2005-2011, the average TCO values remain almost stationary between 259 DU and 260 DU, in the following years it shows an intense decrease until reaching the lowest value, 254 DU in the years 2018, 2019 and 2020. This annual cycle is observed along higher latitudes, however with greater variations as shown in [31].

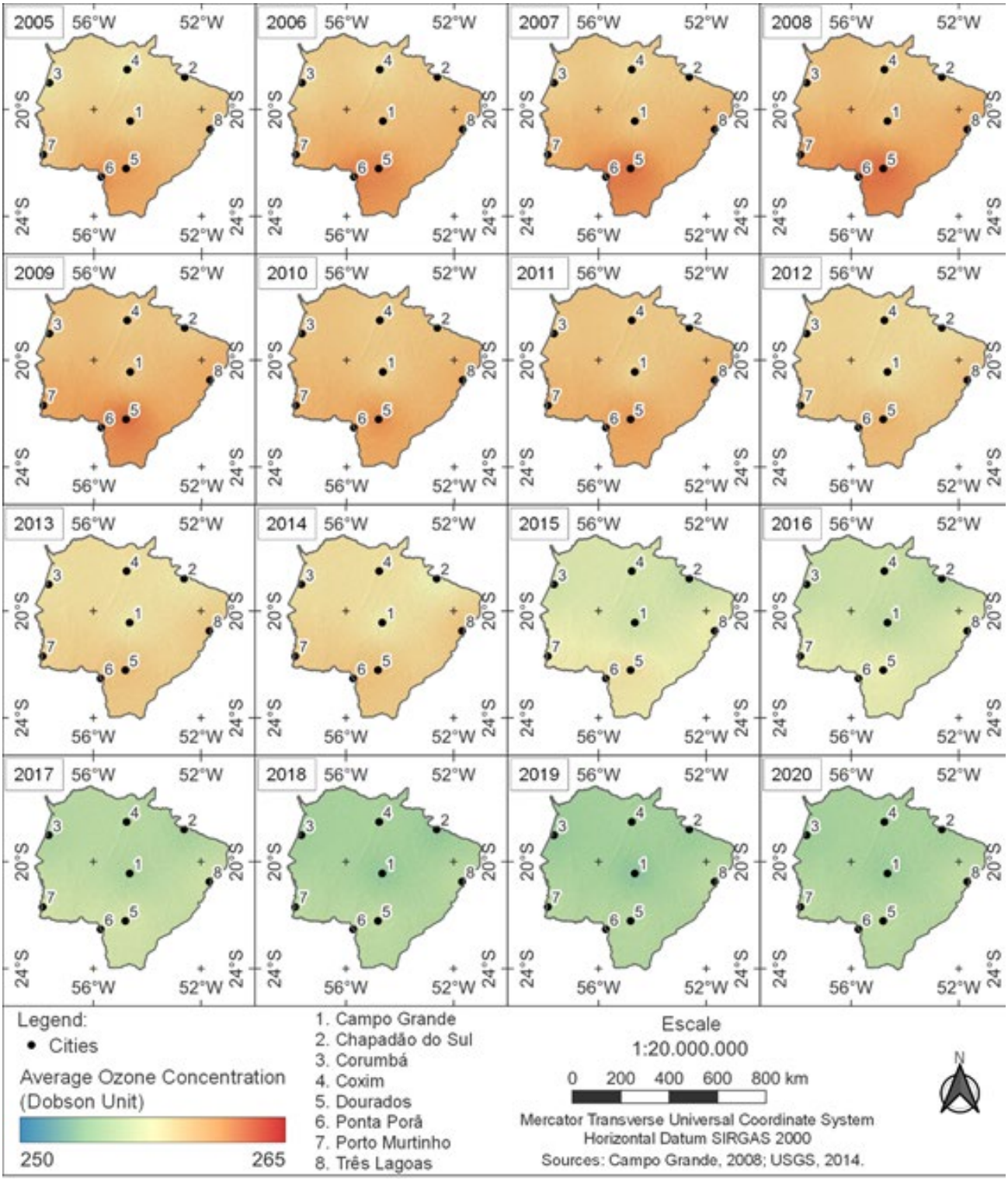

Figure 2 - Spatial and temporal distribution of TCO (DU) for the state of Mato Grosso do Sul from 2005 to 2020.

Analysis of Rainfall Anomaly Indices

To understand the participation of ENSO phenomena in the total annual precipitation of the series presented, the RAI adapted by was applied [2, 3]. The RAI classification is performed following the values described by [27]. Figure 3 shows the estimated RAI for the series of each of the eight regions, which allows classifying the years according to the proposal of (Table 2), and thus obtain the framing of the years in Table 2 [2, 3].

In the analysis of the data from the historical series (2005 to 2020), for the 8 rainfall stations studied and distributed, the RAI are observed for each location. According to this region has a certain climatic uniformity with regard to atmospheric mechanisms (mainly the circulation of air masses), which makes regional thermal diversification due to geographic factors such as altitude, latitude and longitude (continentality) [32]. The same author states that all static climatic factors, such as relief, act on the climate of a given region in interaction with the regional systems of atmospheric circulation, which demonstrates the importance of knowing the circulation systems that act in the region along the of the year to understand the climate.

The dynamics of the study area

Regarding the seasonal and spatial distribution of rainfall, Reboita et al. states that these are very simple, as the topography characteristics do not offer great barriers to the atmospheric circulation systems, which define the rainfall in the Brazilian Center-West Region these precipitations are not evenly distributed throughout the year [32]. In almost all regions, more than 70% of the total precipitation accumulated during the year is from November to March, with the November-January quarter being generally the wettest. On the contrary, the winter is excessively dry and at this time of year the rains are very rare, with an average of 4 to 5 days of occurrence of this phenomenon per month, being even scarcer in the western sector of MS, where at least one month does not record a single day of rain. Therefore, drought occurs most frequently in the June-July-August winter quarter believe that only topographic factors do not play a conditioning role in the spatial distribution of these variables since the atmospheric circulation conditions are practically the same for the entire state of MS. On a macroscale, the main air masses that influence the seasonal variation and distribution of rainfall in the region are the Tropical Atlantic and Polar Atlantic (in winter) and the Tropical Atlantic Mass (in summer) [2, 3, 23].

The rainy season (October to March/April) concentrates over 85% of annual rainfall, with December and January contributing over 35% of annual rainfall. The rainy season (October to March/April) concentrates over 85% of annual rainfall, with December and January contributing over 35% of annual rainfall. The dry season, which begins in April and extends until the beginning of October, is characterized by a significant reduction in rainfall. In the driest quarter of the year (June-August), precipitation represents, on average, less than 2% of the annual total the daily evapotranspiration (ET) and that does not change the dryness of the environment. These periods usually exceed 100 days.

During the period of analysis, the average number of consecutive days in which prolonged droughts occurred did not exceed 75 consecutive days, with the average number of days without significant rainfall (less than 2.5 mm) being 110 days and that almost half of the years has a long period without rain of more than 75 uninterrupted days. This period coincides with the dry season, being more common in the months of June, July and August, reaching until mid-September state of MS [2, 3, 23].

Table 2 shows that after the application of the RAI, 5.7% of the years were considered extremely humid [RAI (4)]. In turn, classified as very humid (2 <RAI <4) are 14.1% of the years and between 0 <RAI <2, that is, wet years, are 32.4%. are 5.0% of the years. In the years classified by the RAI as very dry (-4 <RAI <-2) are 17.2% and the dry RAI (-2 <RAI <0) 5.7%. Finally, the years without anomalies correspond to 3.4%. The years 2004, 2005 and 2006 (normal years) were classified by the RAI as "very dry" (-4.0 < RAI < -2.0). In 2004, 2005 and 2006, the behavior of precipitation should not be scarce, as they are under the neutrality of the ENSO phenomenon, minimum of 72 mm.

The analysis phase of the occurrence of ENSO climate variability mode was for the period 2005-2020. For this, the graphs in Figure 3 show the annual RAI+ and RAI- together with their linear trend line and the standard deviation of the series (supplementary Figure 2).

In Figure 3, it is also possible to identify years that presented precipitation within the standard deviation of the series, considered years with normal precipitation and that were under the influence of the ENSO climate variability mode, both in its positive and negative phases. The classification of the ENSO climate variability mode in years with annual precipitation totals within the standard deviation of the series: 2000; 2001; 2007; 2008; 2010 and 2011 - La Niña and the years: 2002; 2005; 2007; 2009; 2010 - El Niño [34].

It is possible to notice that the adoption of the standard deviation of the series as a method of verifying the influence of ENSO in the annual totals of precipitation for MS, cannot represent, with great precision, the behavior of the phenomenon, mainly in relation to the years with low annual precipitation volumes (negative phase of the phenomenon) [2, 3].

Climatic anomalies can last several months, mainly in the tropical atmosphere, and are not only characterized by the lack or excess of some meteorological element, but also imply a change in their temporal and spatial distribution. On a global scale, the greatest influence is due to the ENSO climate variability mode and its different phases/intensities (El Niño -EN; La Niña -LN), which are closely related to changes in climate, atmospheric circulation

configurations and ocean-atmosphere interaction in the Pacific and Atlantic oceans thus determining air temperature anomalies and especially rainfall in various regions [32, 35]. ENSO can mainly influence the change in the regional rainfall regime, which can result in severe droughts or extreme rainfall, significantly interfering with human activities and alternating rainy and dry periods.

In general, the impacts of El Niño and La Niña events are known to have spatial and temporal variability, with long periods with consistent continuous anomalies not being observed at the regional scale [36]. According to Souza et al. (2013) the total monthly and annual variations in precipitation are due to the behavior of the regional atmospheric circulation throughout the year, together with local or regional geographic factors, the atmospheric systems operating in Mato Grosso do Sul are: Intertropical Convergence Zone (ITCZ), Equatorial Zone Continental Tropical System (EZCTS), Atlantic Tropical System (STA), Atlantic Polar System (APS) and South Atlantic Convergence Zone (SACZ) [2, 3, 34].

The characterization of dry winters and rainy summers in Central-West Brazil stems from the stability generated by the influence of the South Atlantic Subtropical Anticyclone (SASA) and the small ridges that form over the South American (SA) continental part. The rainy season is associated with the southward shift of the ITCZ, following the apparent movement of the sun towards the Tropic of Capricorn (summer). Over the central portion of SA, the CIT advances further south than in coastal regions, generating instability throughout central Brazil in the summer months. Due to the influence of the tropical marine and equatorial air mass, temperatures are high throughout the year. In winter, when the ITCZ is shifted to the north, the region has low or no precipitation (Oliveira Júnior et al. 2021). According to Souza et al. (2013) an important climatic factor that acts in the state of MS and alters rainfall levels is altitude, which allows for differences in thermal and rainfall conditions between nearby locations (distances less than 100 km from each other).

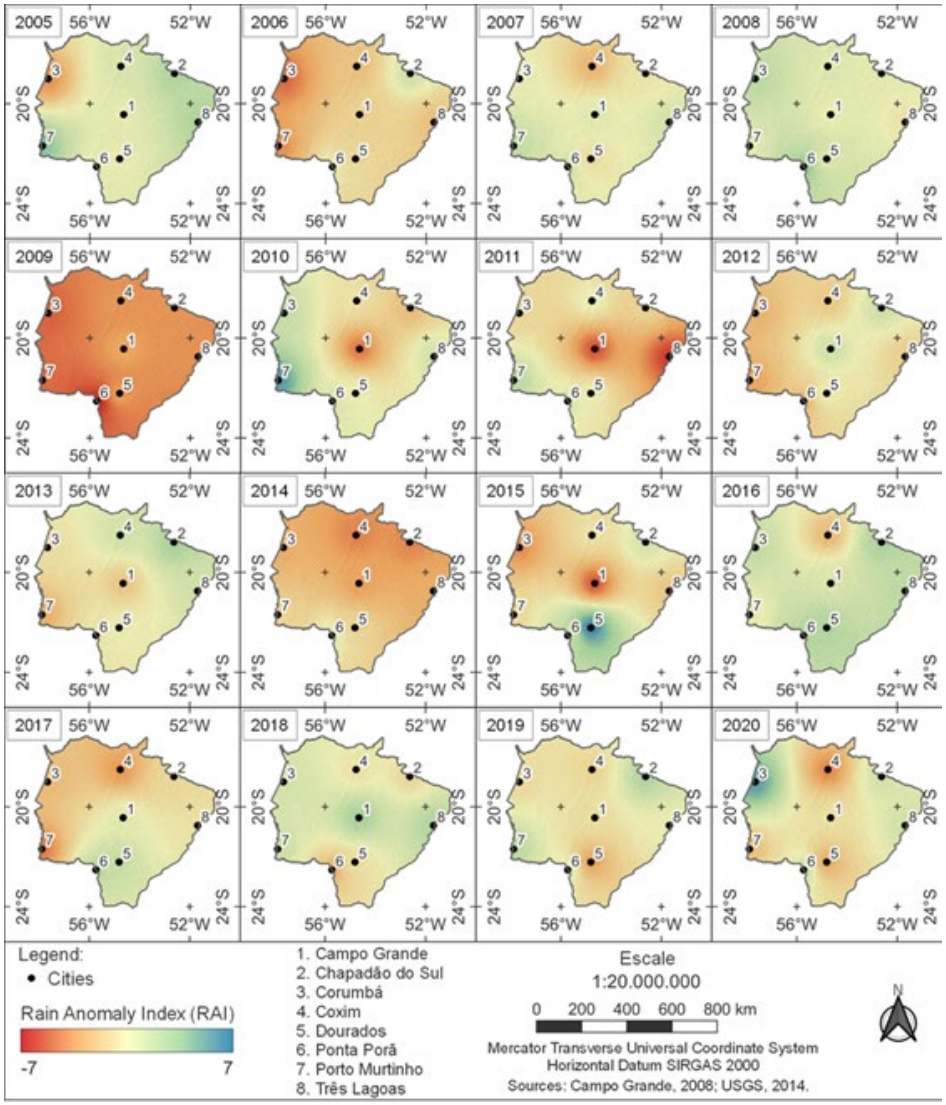

Figure 3 - Spatial and temporal distribution of RAI+ and RAI- for the state of Mato Grosso do Sul from 2005 to 2020.

Figure 4 shows the correlation (*r*) and p values for the correlation between ozone and RAI+ and RAI -, for Mato Grosso do Sul. Pearson's correlation coefficients range from -0.94 (Coxim) to -0.54 (Gold), for RAI - and ozone at 5% error probability ($r \neq 0$) and for RAI+ and ozone they ranged from -0.93 (Ponta Pora) to -0.70 (Corumba).

The weak correlation indicates little influence of the El Niño and La Niña phenomena on the O_3 of Mato Grosso do Sul. However, here there can often be a delay in the response of the precipitation index to the occurrence of ENSO and in the O_3 column, which may, in part, explain the low correlations.

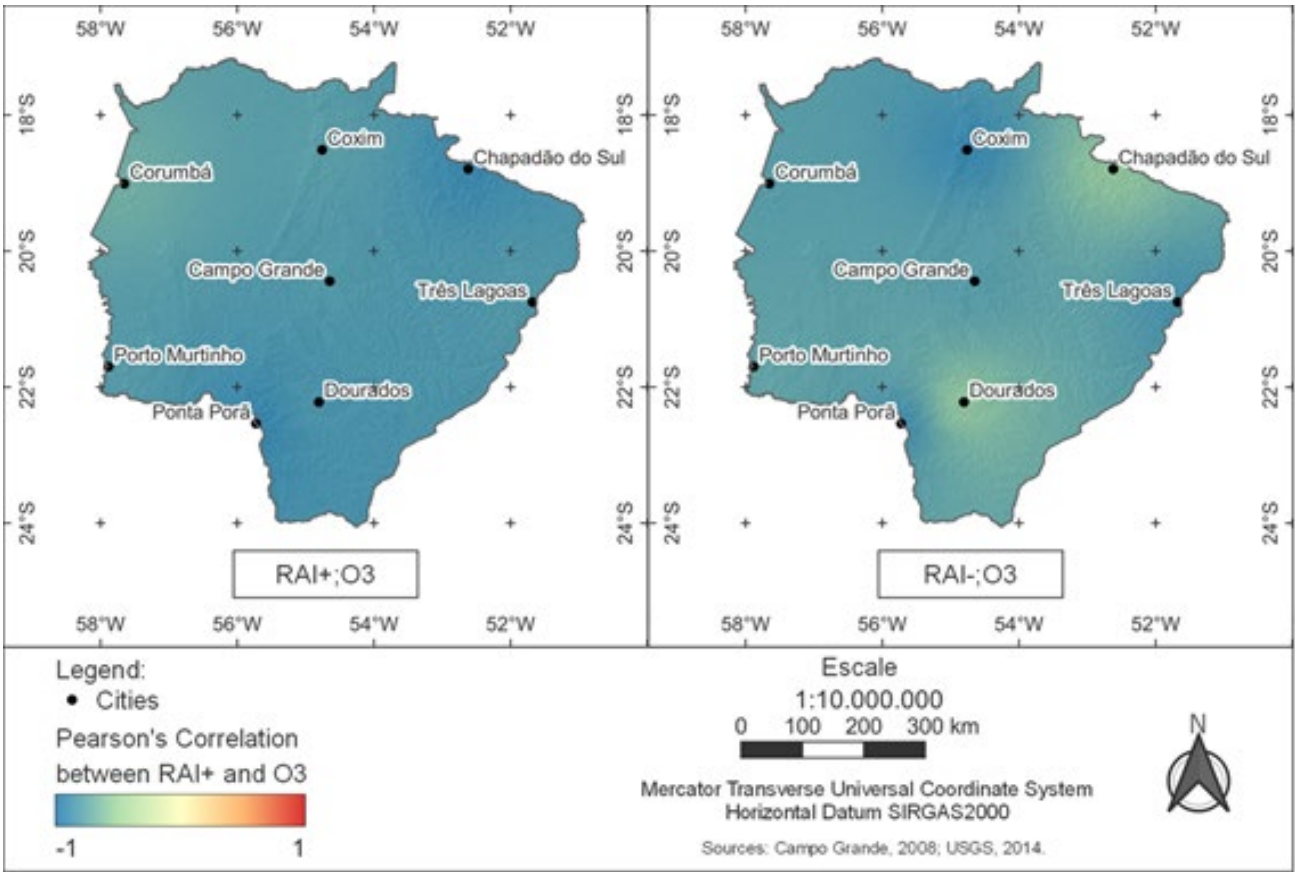

Figure 4: Spatial distribution of correlations between RAI+ and ozone column and RAI- and ozone column for the state of Mato Grosso do Sul from 2005 to 2020.

Influence of ENSO on the Interannual Variability of TCO in MS

The variability of TCO for the period from 2005 to 2020 in the MS region is shown in Fig. 2, where it is possible to observe the TCO values with a variation of ~2.5% in the region. The most significant variations occur in the period between August and November, a period in which there is a significant increase in TCO averages in the mid-latitudes regions due to the presence of the Antarctic Polar Vortex, which acts as a barrier preventing the arrival of the contents of ozone distributed by the CBD in the polar region, and thus, the ozone contents are trapped in the mid-latitudes region similar to what was exposed in (Dias Nunes et al. 2020). From April to May all latitudes show a decrease in mean values.

Observed Tropospheric Ozone Response to La Niña

Higher tropospheric ozone levels are evident at mid-latitudes, (Figure 1), mainly due to higher emission of ozone precursors Lamarque et al. [37]. To determine the relationship between MS satellite-derived tropospheric column and La Niña events, we compared the La Niña index and ozone anomaly time series. There were six La Niña and five El Niño events during 2005-2020 (see supplementary material, supplementary), implying that the irregular occurrence of ENSO does not significantly affect ozone levels. MS ozone concentration shows considerable interannual variability with a standard deviation of 2.36 DU and appears to be behind the La Nina index by a few months, implying that the mechanism of O3 variation may be associated with ENSO.

To verify the spatial distribution of O_3, we evaluated the regression of tropospheric column ozone in relation to the La Niña index (supplementary material 3). A slight increase/decrease in tropospheric column ozone is observed with an average regression coefficient: R^2=0.88 for Ponta Porã (RAI+) and a smaller R^2=0.32 for

Chapadão do Sul (RAI-) (supplementary Figures 3 and 4). Thus, ENSO can be considered the main driver of interannual variability in TCO over MS; higher and lower levels of O_3 are associated with La Niña and El Niño, respectively.

As we used the linear regression method, the ozone anomalies associated with El Niño would resemble those of La Niña, but with opposite signs. In other words, El Nin leads to a decrease in tropospheric column ozone. This indicates that anthropogenic emission trends alone are not sufficient to unambiguously attribute ozone trends to global climate change, because each ENSO event has unique appearances Timmermann et al., and ENSO has been changing [39].

El Niño Effects on the Troposphere

ENSO also has a major influence on the interannual variability of troposphere chemistry [40]. Studies of the impact of ENSO on composition (ozone and precursors) in the tropical region found an increase in tropospheric O3 column in the western Pacific and over Indonesia in El Niño years associated with dryness, downward motion and suppressed convection [41]. High tropospheric ozone levels can be observed, coincident with fires over MS during El Niño-induced drought conditions. This increase is of interest in the impact of ENSO on tropospheric ozone, particularly in relation to atmospheric dynamics compared to the increase in biomass burning during El Niño, it can be observed that fires increase during El Niño events with an even greater increase during El Niño events extreme events. So far, the measured and simulated tropospheric ozone column anomaly patterns for El Niño have been quite consistent, showing an increase over MS. These changes in TCO are attributed to a combination of large-scale circulation processes associated with changing Walker cell convection patterns and surface/boundary layer processes due to forests in MS biomes. Changes in circulation cause a decrease in TCO associated with increased convection and upward movement of low-ozone air from the lower troposphere, and an increase associated with suppressed convection and downward movement of ozone-rich air from the upper troposphere Doherty et al. [40]. In addition to the anti-correlation between TCO anomalies and convection changes, Sudo and Takahashifound that there are other chemical changes occurring during El Niño, changes in specific humidity, cloud mass flow, and wind impact the chemical lifetime of O_3 [10, 11]. In the atmosphere the troposphere decreased humidity results in an increase in O3 lifespan and vice-versa.

Wei et al. studied the ENSO in Asia, using satellite measurements of tropospheric column ozone and chemical-climate model simulations, found that observed ozone tends to increase in the East Asian troposphere 4 months after the La Niña peak [41]. These post-La Niña changes are also evident in the results of the chemical-climate model, albeit with a slightly longer delay (5 months).

Lima et al. analyzed the annual variation and effects of the El Niño atmospheric variability mode (Canonical and Modoki) on the TCO over Northeast Brazil (NEB) between 1997 and 2018 using data from Total Ozone Mapping Sensors Spectrometer (TOMS) and OMI [28]. There was an average monthly variation throughout the studied area with typical behavior of the annual cycle in seasonal variability, with a minimum value in May and a maximum in October. A downward trend was observed in the series of mean values during the analyzed period. The averages of the anomalies show that El Niño events affect the TCO, predominantly causing a decrease in its values. These events in Modoki mode have greater potential to affect the TCO than Canonicals with negative anomalies of greater intensity.

Yang et al. studied different impacts of hot/cold phases of ENSO on summer tropospheric O_3 over China based on model simulations, soil measurements and reanalysis data [42]. Summer surface O_3 concentrations in China show a positive correlation with the ENSO index during the years 1990-2019, with the largest increases of 20% in southern China in El Niño (warm phase) versus La Niña years (cold phase). Furthermore, the increase in O_3 during El Niño years is mainly due to domestic emissions in China. This study highlights the potential significance of ENSO in modulating tropospheric O_3 concentrations in China, with major implications for the mitigation of O_3 pollution.

Conclusions

Considering that ozone controls atmospheric oxidizing capacity, understanding the influence of ENSO on tropospheric ozone variability is essential to unravel its complex climate-chemical interactions. In general, ENSO modulates atmospheric circulation, however, there is insufficient evidence of tropospheric ozone changes due to ENSO-induced circulations.

• Ozone increases over the MS region during El Niño events and decreases during La Niña events.

• ENSO may be one of the main drivers of tropospheric column ozone variability in MS. First, observational analysis revealed that tropospheric column ozone tends to increase after La Nina peaks, along with the anomalies and descenders that provide favorable weather conditions for ozone transport. It should also be noted that the properties of ENSO are continuously changing under greenhouse warming. Thus, the effects of ENSO on tropospheric ozone may change, which is an interesting question to be resolved [43].

Consent to Participate: All authors declare their consent to participate in the article.

Funding: This research did not receive any external funding.

Competing Interests: The authors declare no conflicts of interest.

Availability of data and materials: This research was supported by the Universities and by the UFMS Air Quality Laboratory.

References

1. Anenberg, S. C., West, J. J., Fiore, A. M., Jaffe, D. A., Prather, M. J., Bergmann, D., ... & Zeng, G. (2009). Intercontinental impacts of ozone pollution on human mortality.
2. de Oliveira, S. S., de Souza, A., Abreu, M. C., de Oliveira Júnior, J. F., & Cavazzana, G. H. (2020). SPACE-TEMPORAL CHARACTERIZATION OF SOUTH MATO GROSSO PRECIPITATION: RAIN DISTRIBUTION AND RAIN ANOMALY INDEX (IAC) ANALYSIS FOR CLIMATE PHENOMENA. Revista Brasileira de Climatologia, 27.
3. de Oliveira-Junior, J. F., Teodoro, P. E., da Silva Junior, C. A., Baio, F. H. R., Gava, R., Capristo-Silva, G. F., ... & da Silva Costa, M. (2020). Fire foci related to rainfall and biomes of the state of Mato Grosso do Sul, Brazil. Agricultural and Forest Meteorology, 282, 107861.
4. Yi, F., McCarl, B. A., Zhou, X., & Jiang, F. (2018). Damages of surface ozone: evidence from agricultural sector in China. Environmental Research Letters, 13(3), 034019.
5. Akimoto, H., Kurokawa, J. I., Sudo, K., Nagashima, T., Takemura, T., Klimont, Z., ... & Suzuki, K. (2015). SLCP co-control approach in East Asia: Tropospheric ozone reduction strategy by simultaneous reduction of NOx/NMVOC and methane. Atmospheric Environment, 122, 588-595.
6. Lelieveld, J., & Dentener, F. J. (2000). What controls tropospheric ozone?. Journal of Geophysical Research: Atmospheres, 105(D3), 3531-3551.
7. Ziemke, J. R., & Chandra, S. (2003). La Nina and El Nino—induced variabilities of ozone in the tropical lower atmosphere during 1970–2001. Geophysical Research Letters, 30(3).
8. Chandra, S., Ziemke, J. R., Min, W., & Read, W. G. (1998). Effects of 1997–1998 El Nino on tropospheric ozone and water vapor. Geophysical Research Letters, 25(20), 3867-3870.
9. Chandra, S., Ziemke, J. R., Duncan, B. N., Diehl, T. L., Livesey, N. J., & Froidevaux, L. (2009). Effects of the 2006 El Niño on tropospheric ozone and carbon monoxide: implications for dynamics and biomass burning. Atmospheric Chemistry and Physics, 9(13), 4239-4249.
10. Sudo, K., & Takahashi, M. (2001). Simulation of tropospheric ozone changes during 1997–1998 El Nino: Meteorological impact on tropospheric photochemistry. Geophysical research letters, 28(21), 4091-4094.
11. Sudo, K., & Takahashi, M. (2001). Simulation of tropospheric ozone changes during 1997–1998 El Nino: Meteorological impact on tropospheric photochemistry. Geophysical research letters, 28(21), 4091-4094.
12. Doherty, R. M., Stevenson, D. S., Collins, W. J., & Sanderson, M. G. (2005). Influence of convective transport on tropospheric ozone and its precursors in a chemistry-climate model. Atmospheric Chemistry and Physics, 5(12), 3205-3218.
13. Lin, M., Horowitz, L. W., Oltmans, S. J., Fiore, A. M., & Fan, S. (2014). Tropospheric ozone trends at Mauna Loa Observatory tied to decadal climate variability. Nature Geoscience, 7(2), 136-143.
14. Olsen, M. A., Wargan, K., & Pawson, S. (2016). Tropospheric column ozone response to ENSO in GEOS-5 assimilation of OMI and MLS ozone data. Atmospheric Chemistry and Physics, 16(11), 7091-7103.
15. Verstraeten, W. W., Neu, J. L., Williams, J. E., Bowman, K. W., Worden, J. R., & Boersma, K. F. (2015). Rapid increases in tropospheric ozone production and export from China. Nature geoscience, 8(9), 690-695.
16. Rowlinson, M. J., Rap, A., Arnold, S. R., Pope, R. J., Chipperfield, M. P., McNorton, J., ... & Siddans, R. (2019). Impact of El Niño–Southern Oscillation on the interannual variability of methane and tropospheric ozone. Atmospheric Chemistry and Physics, 19(13), 8669-8686.
17. Rodrigues, R. R., Campos, E. J., & Haarsma, R. (2015). The impact of ENSO on the South Atlantic subtropical dipole mode. Journal of Climate, 28(7), 2691-2705.
18. Zhang, J., Tian, W., Wang, Z., Xie, F., & Wang, F. (2015). The influence of ENSO on northern midlatitude ozone during the winter to spring transition. Journal of Climate, 28(12), 4774-4793.
19. Diallo, M., Konopka, P., Santee, M. L., Müller, R., Tao, M., Walker, K. A., ... & Ploeger, F. (2019). Structural changes in the shallow and transition branch of the Brewer–Dobson circulation induced by El Niño. Atmospheric chemistry and physics, 19(1), 425-446.
20. Xie, F., Li, J., Tian, W., Feng, J., & Huo, Y. (2012). Signals of El Niño Modoki in the tropical tropopause layer and stratosphere. Atmospheric Chemistry and Physics, 12(11), 5259-5273.
21. Manatsa, D., & Mukwada, G. (2017). A connection from stratospheric ozone to El Niño-Southern Oscillation. Scientific Reports, 7(1), 1-10.
22. Xie, F., Li, J., Tian, W., Zhang, J., & Sun, C. (2014). The relative impacts of El Niño Modoki, canonical El Niño, and QBO on tropical ozone changes since the 1980s. Environmental Research Letters, 9(6), 064020.
23. Teodoro, P. E., de Oliveira-Júnior, J. F., Da Cunha, E. R., Correa, C. C. G., Torres, F. E., Bacani, V. M., ... & Ribeiro, L. P. (2016). Cluster analysis applied to the spatial and temporal variability of monthly rainfall in Mato Grosso do Sul State, Brazil. Meteorology and Atmospheric Physics, 128(2), 197-209.
24. Souza, A. D., Fernandes, W. A., Albrez, E. D. A., & Galvíncio, J. D. (2012). Análise de agrupamento da precipitação e da temperatura no Mato Grosso do Sul. Acta Geográfica, 6(12), 109-24.
25. Alvares, C. A., Stape, J. L., Sentelhas, P. C., Gonçalves, J. D. M., & Sparovek, G. (2013). Köppen's climate classification map for Brazil. Meteorologische Zeitschrift, 22(6), 711-728.
26. Levelt, P. F., Hilsenrath, E., Leppelmeier, G. W., van den Oord, G. H., Bhartia, P. K., Tamminen, J., ... & Veefkind, J. P. (2006). Science objectives of the ozone monitoring instrument. IEEE Transactions on Geoscience and Remote Sensing, 44(5), 1199-1208.
27. Brito, A. P. D., Silva, N. C. D., Tomasella, J., Ferreira, S. J.

F., & Monteiro, M. T. F. (2022). Analysis of the Rain Anomaly Index and Precipitation Trend for Pluviometric Stations in Central Amazonia. Revista Brasileira de Meteorologia.
28. Lima, D. M. C. D., Nunes, M. D., & Mariano, G. L. (2021). Impacto do ENOS na Variabilidade da Coluna Total de Ozônio Sobre a Região Nordeste do Brasil-Parte 1: El Niño Canônico e Modoki. Revista Brasileira de Meteorologia, 35, 931-944.
29. Lopo, A. B., Spyrides, M. H. C., Lucio, P. S., & Sigró, J. (2013). Radiação ultravioleta, ozônio total e aerossóis na cidade de Natal-RN. Holos, 6, 3-21.
30. Sousa, C. T., Leme, N. M. P., Martins, M. P. P., Silva, F. R., Penha, T. L. B., Rodrigues, N. L., ... & Hoelzemann, J. J. (2020). Ozone trends on equatorial and tropical regions of South America using Dobson spectrophotometer, TOMS and OMI satellites instruments. Journal of Atmospheric and Solar-Terrestrial Physics, 203, 105272.
31. Nunes[1], M. D., Mariano, G. L., & Alonso, M. F. (2020). Variabilidade espaço-temporal da coluna total de ozônio e sua relação com a radiação ultravioleta na América do Sul. Revista Brasileira de Geografia Física, 13(05), 2053-2073.
32. Reboita, M. S., Gan, M. A., Rocha, R. P. D., & Ambrizzi, T. (2010). Regimes de precipitação na América do Sul: uma revisão bibliográfica. Revista brasileira de meteorologia, 25, 185-204.
33. Souza, A. P., Mota, L. L., Zamadei, T., Martin, C. C., Almeida, F. T., & Paulino, J. (2013). Classificação climática e balanço hídrico climatológico no estado de Mato Grosso. Nativa, 1(1), 34-43.
34. de Oliveira-Júnior, J. F., da Silva Junior, C. A., Teodoro, P. E., Rossi, F. S., Blanco, C. J. C., Lima, M., ... & dos Santos Vanderley, M. H. G. (2021). Confronting CHIRPS dataset and in situ stations in the detection of wet and drought conditions in the Brazilian Midwest. International Journal of Climatology, 41(9), 4478-4493.
35. Lyra, G. B., Oliveira-Júnior, J. F., Gois, G., Cunha-Zeri, G., & Zeri, M. (2017). Rainfall variability over Alagoas under the influences of SST anomalies. Meteorology and Atmospheric Physics, 129(2), 157-171.
36. de Gois, G., Delgado, R. C., & de Oliveira Júnior, J. F. (2015). Modelos teóricos transitivos aplicados na interpolação espacial do Standardized Precipitation Index (SPI) para os episódios de El Niño forte no Estado do Tocantins, Brasil. Irriga, 20(2), 371-387.
37. Lamarque, J. F., Bond, T. C., Eyring, V., Granier, C., Heil, A., Klimont, Z., ... & Van Vuuren, D. P. (2010). Historical (1850–2000) gridded anthropogenic and biomass burning emissions of reactive gases and aerosols: methodology and application. Atmospheric Chemistry and Physics, 10(15), 7017-7039.
38. Yeh, S. W., Cai, W., Min, S. K., McPhaden, M. J., Dommenget, D., Dewitte, B., ... & Kug, J. S. (2018). ENSO atmospheric teleconnections and their response to greenhouse gas forcing. Reviews of Geophysics, 56(1), 185-206.
39. Cai, W., Wang, G., Dewitte, B., Wu, L., Santoso, A., Takahashi, K., ... & McPhaden, M. J. (2018). Increased variability of eastern Pacific El Niño under greenhouse warming. Nature, 564(7735), 201-206.
40. Doherty, R. M., Stevenson, D. S., Johnson, C. E., Collins, W. J., & Sanderson, M. G. (2006). Tropospheric ozone and El Niño–Southern Oscillation: Influence of atmospheric dynamics, biomass burning emissions, and future climate change. Journal of Geophysical Research: Atmospheres, 111(D19).
41. Wie, J., Moon, B. K., Yeh, S. W., Park, R. J., & Kim, B. G. (2021). La Niña-related tropospheric column ozone enhancement over East Asia. Atmospheric Environment, 261, 118575.
42. Yang, Y., Li, M., Wang, H., Li, H., Wang, P., Li, K., ... & Liao, H. (2022). ENSO modulation of summertime tropospheric ozone over China. Environmental Research Letters, 17(3), 034020.
43. Thompson, A. M., Witte, J. C., Hudson, R. D., Guo, H., Herman, J. R., & Fujiwara, M. (2001). Tropical tropospheric ozone and biomass burning. Science, 291(5511), 2128-2132.